Kinetic and Structural Studies of the Reactions of Phosphorous Nucleophiles with the Sulfido Bimetallic Clusters $Cp'_2Mo_2Co_2S_3(CO)_4$ and $Cp'_2Mo_2Co_2S_4(CO)_2$. X-ray Crystal Structure of $Cp'_2Mo_2Co_2S_3(CO)_4(PMe_3)$

Owen J. Curnow,† Jeff W. Kampf,† M. David Curtis,*,† Jian-Kun Shen,‡ and Fred Basolo*,‡

Contribution from the Departments of Chemistry, The University of Michigan, Ann Arbor, Michigan 48109-1055, and Northwestern University, Evanston, Illinois 60208-3113

Received August 19, 1993®

Abstract: The syntheses of the carbonyl substituted clusters $Cp'_2Mo_2Co_2S_3(CO)_{4-n}L_n$, n = 1, 2, Cp' = η^5-C_5H_4Me, L = PPh_3, P(n-Bu)$_3$, P(OMe)$_3$, PPh_2H, and $PPhH_2$, are described. Kinetic studies were performed that show the CO substitution involves two elementary steps; an adduct is formed in a preequilibrium step, followed by CO dissociation from the adducts. Equilibrium constants and CO-dissociation rate constants were obtained. The formation of the initial adduct is associative. Typical activation parameters are $\Delta H^\ddagger$ = 24 ± 3 kcal/mol, $\Delta S^\ddagger$ = 0 ± 8 eu for CO dissociation and $\Delta H^\ddagger$ = 6 kcal/mol, $\Delta S^\ddagger$ = −28 eu for associative adduct formation with PPh_3. Substitution of CO by PPh_3 on the cubane cluster $Cp'_2Mo_2Co_2S_4(CO)_2$ is also associative. $\Delta H^\ddagger$ = 11.3 ± 0.8 kcal/mol, $\Delta S^\ddagger$ = −24 ± 3 eu. With Me_3P, the adduct $Cp'_2Mo_2Co_2S_3(CO)_4(PMe_3)$ was isolated and its crystal structure determined by X-ray crystallography: monoclinic, space group = Pn (no. 7), a = 7.089(1) Å, b = 18.669(6) Å, c = 18.469(4) Å, β = 90.84(2)°, Z = 4, d = 2.04 g cm^{-3}, R = 0.040, R_w = 0.050, GOF = 1.42 based on 4739 reflections with $F \geq 5\sigma(F)$ and 533 refined parameters. The molecule consists of a slightly folded Co_2Mo_2 butterfly with a Mo–Mo bond at the hinge (hinge angle = 148°). The $Mo_2Co(CO)_2$ triangle has two μ_3-bridging sulfide ligands, while the $Mo_2Co(CO)_2$-(PMe_3) triangle has one μ_3-S. Some bond distances are Mo–Mo, 2.594(2) Å; Mo–Co, 2.692–2.813 Å; Mo–S, 2.38 Å; Co–S, 2.16 Å.

Introduction

We have recently reported that the Mo/Co/S cluster **1** reacts with organic thiols to give the cubane cluster **2** and the corresponding alkane in a reaction related to hydrodesulfurization (HDS) catalysis (eq 1).[1] Despite various attempts, we were unable

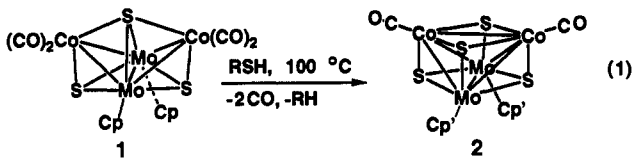

1 2 (1)

to isolate or detect any intermediates formed in the course of the reaction. It appeared that the slow step was the initial coordination of the thiol to the cluster, and the ensuing desulfurization and decarbonylation steps were sufficiently rapid that the concentrations of any intermediates remained very low.

We then investigated the reactions of **1** with phosphines that are more nucleophilic than the thiols with the hope that the change in relative rates of substitution vs element abstraction and/or decarbonylation would allow detection of intermediates and allow us to gain some insight into the element abstraction mechanism.[2,3] Kinetic studies on ligand substitution reactions of metal carbonyl clusters are interesting in several respects.[4] These include metal triad effects,[5] phosphorous ligand (ligand on the metal in cluster complexes or as entering ligand) effects,[4b,6] high nuclearity effects,[7] chemical assisted reactions,[8,9] etc. Despite much study, little kinetic information is available to evaluate heteroatom effects on the reactivities of metal clusters, although tremendous effort has been made in the synthesis and structural characterization of such complexes.[10]

A previous kinetic study showed that $Fe_3S_2(CO)_9$ undergoes CO substitution by a dissociative mechanism,[11] but $FeCo_2S(CO)_9$ reacts by parallel dissociative and associative pathways, with the latter predominating with good nucleophiles.[12] In other cases, nucleophilic attack on metal carbonyl clusters has yielded edge-opened clusters by breaking a metal–metal bond.[13,14] In fact, metal–metal bond cleavage is much more common than metal–heteroatom bond breaking in associative substitution reactions on clusters,[13] although a few instances are recorded where a metal–ligand bond is displaced instead.[15-17] Since an X-ray crystal

† The University of Michigan.
‡ Northwestern University.
• Abstract published in *Advance ACS Abstracts*, December 1, 1993.

(1) Riaz, U.; Curnow, O.; Curtis, M. D. *J. Am. Chem. Soc.* **1991**, *113*, 1416.
(2) Curnow, O. J.; Kampf, J. W.; Curtis, M. D. *Organometallics* **1991**, *10*, 2546.
(3) Curnow, O. J.; Kampf, J. W.; Curtis, M. D.; Mueller, B. L. *Organometallics* **1992**, *11*, 1984.
(4) (a) Poë, A. J. In Metal Clusters; Moskovits, M., Ed.; Wiley: New York, 1986; Chapter 4, p 53. (b) Basolo, F. *Polyhedron* **1990**, *9*, 1503. (c) Poë, A. J. *Pure Appl. Chem.* **1988**, *60*, 1209.
(5) (a) Kennedy, J. R.; Selz, P.; Rheingold, A. L.; Trogler, W. C.; Basolo, F. *J. Am. Chem. Soc.* **1989**, *111*, 3615. (b) Kennedy, J. R.; Basolo, F.; Trogler, W. C. *Inorg. Chim. Acta* **1988**, *146*, 75.
(6) Atwood, J. D.; Wovkulich, M. J.; Sonnenberger, D. C. *Acc. Chem. Res.* **1983**, *16*, 350.
(7) Poë, A. J.; Farrar, D. H.; Zheng, Y. *J. Am. Chem. Soc.* **1992**, *114*, 5146.
(8) Shen, J. K.; Shi, Y. L.; Gao, Y. C.; Shi, Q. Z.; Basolo, F. *J. Am. Chem. Soc.* **1988**, *110*, 2414.
(9) Lavigne, G.; Kaesz, H. D. *J. Am. Chem. Soc.* **1984**, *106*, 4647.
(10) Shriver, D. F.; Kaesz, H. D.; Adams, R. D. *The Chemistry of Metal Cluster Complexes*; VCH: New York, 1990.
(11) Cetini, G.; Stanghellini, P. L.; Rossetti, R.; Gambino, O. *Inorg. Chim. Acta* **1968**, *2*, 433.
(12) Rossetti, R.; Gervasio, G.; Stanghellini, P. L. *J. Chem. Soc., Dalton Trans.* **1978**, 222.
(13) Albers, M. O.; Robinson, D. J.; Coville, N. J. *Coord. Chem. Rev.* **1986**, *69*, 127.
(14) Adams, R. D.; Chi, Y.; DesMarteau, D. D.; Lentz, D.; Marschall, R.; Scherrmann, A. *J. Am. Chem. Soc.* **1992**, *114*, 10822.
(15) Darchen, A.; Lhadi, E. K.; Patin, H. *J. Organomet. Chem.* **1989**, *363*, 137.
(16) Ohst, H. H.; Kochi, J. K. *J. Am. Chem. Soc.* **1986**, *108*, 2897.
(17) Johnson, B. F. G.; Lewis, J.; Pippard, D. A. *J. Organomet. Chem.* **1981**, *213*, 249.

0002-7863/94/1516-0224$04.50/0 © 1994 American Chemical Society

structure determination on the PMe_3 adduct of **1** showed that the phosphine ligand had attached to one of the Co atoms with breakage of the Co–(μ_4-S) bond, a more complete kinetic study of these reactions was desirable. In this paper, we report the results of our kinetic and structural investigations of the reactions of clusters **1** and **2** with phosphorous nucleophiles.

Experimental Section

Unless specified otherwise, all reagents were obtained from Aldrich Co. PPh_2H, P(*n*-Bu)$_3$, and P(OMe)$_3$ were distilled over sodium under a nitrogen atmosphere before use. PPh_3 was purified by recrystallization from ethyl alcohol. $Cp'_2Mo_2Co_2S_3(CO)_4$ and $Cp'_2Mo_2Co_2S_4(CO)_2$ were synthesized by literature methods.[18,19] Decalin was refluxed over sodium and distilled under an atmosphere of nitrogen. Toluene, diethyl ether, and tetrahydrofuran (THF) were distilled under nitrogen from Na/benzophenone; dichloromethane and hexane were similarly distilled from CaH_2. All manipulations of air- or moisture-sensitive compounds were carried out in an inert atmosphere box or by use of Schlenk line techniques. ^{1}H- and ^{13}C-NMR spectra were collected on a Bruker AM-300 or a Bruker WM-360 instrument. ^{31}P-NMR spectra were obtained on a GE GN-500 NB spectrometer. IR spectra were recorded on a Nicolet 5-DXB instrument, and mass spectra were obtained on a Finnegan 4021 quadrupole spectrometer. Elemental analyses were performed by Spang, Galbraith, ORS, or the University of Michigan microanalytical laboratories.

Reaction of $Cp'_2Mo_2Co_2S_3(CO)_4$ with P(OMe)$_3$. A solution of $Cp'_2Mo_2Co_2S_3(CO)_4$ (100 mg, 0.15 mmol) with P(OMe)$_3$ (0.3 mL, 2.5 mmol) in 10 mL of toluene was kept at 30 °C for 3 h. The solvent was removed under vacuum at room temperature, and the residue was dissolved in 1 mL of THF. Pentane (5 mL) was slowly added to the THF solution, which was then cooled to –20 °C. A mixture of *trans*- and *cis*-$Cp'_2Mo_2Co_2S_3(CO)_2[P(OMe)_3]_2$ was obtained as dark brown crystals. IR of the mixture (decalin): 1927, 1940, 1949 cm^{-1}. Anal. Calcd for $C_{20}H_{32}Co_2Mo_2O_8P_2S_3$: C, 27.66; H, 3.68. Found: C, 28.43; H, 3.87. ^{1}H-NMR (C_6D_6): trans, 5.78 (m, 2H), 5.73 (m, 2H), 5.54 (m, 2H), 5.34 (m, 2H), 3.39 (d, J_{PH} = 12Hz, 18H), 2.11 (s, 6H); cis, 5.89 (t, 2H), 5.59 (t, 2H), 5.44 (t, 2H), 5.27 (t, 2H), 3.42 (d, J_{PH} = 12Hz, 18H), 2.22 (s, 3H), 2.07 (s, 3H).

The mother liquor from $Cp'_2Mo_2Co_2S_3(CO)_2[P(OMe)_3]_2$ was collected, and the solvent was removed under vacuum. The residue was extracted with pentane at –20 °C. The pentane solution was concentrated and cooled to –78 °C to give the monosubstituted cluster $Cp'_2Mo_2Co_2S_3(CO)_3P(OMe)_3$ as brown powder. IR ν(CO) in decalin: 1993, 1948 cm^{-1}. A compound believed to be the adduct $Cp'_2Mo_2Co_2S_3(CO)_3[P(OMe)_3]_2$ is formed upon adding P(OMe)$_3$ to $Cp'_2Mo_2Co_2S_3(CO)_3P(OMe)_3$ solution in decalin. IR: ν(CO) 1965, 1947, 1929 cm^{-1}. This compound is converted to the disubstituted complex, $Cp'_2Mo_2Co_2S_3(CO)_2[P(OMe)_3]_2$, when the solution is kept at 30 °C for 24 h.

$Cp'_2Mo_2Co_2S_3(CO)_3(PPhH_2)$. $Cp'_2Mo_2Co_2S_3(CO)_4$ (0.281 g, 0.416 mmol) was dissolved in 30 mL of toluene. $PPhH_2$ (0.4 mL, 1.36 mmol) was added by syringe and the solution stirred for 8 days. Chromatography down a 25-cm column of alumina with 1:1 toluene/hexane eluted a small amount of $Cp'_2Mo_2Co_2S_3(CO)_4$ followed by a dark brown band of $Cp'_2Mo_2Co_2S_3(CO)_3(PPhH_2)$ (0.20 g, 65% yield), which was eluted with a 3:1 toluene/hexane solution. A small green band was not eluted. ^{1}H-NMR (C_6D_6): δ 7.55 (m, 2H, Ph*H*), 7.03 (m, 3H, Ph*H*), 5.43 (m, 2H), 5.30 (m, 1H), 5.15 (m, 1H), 5.11 (m, 2H), 4.80 (m, 1H), 4.62 (m, 1H) 2ABCD pattern for Cp*H*, 4.99 (dd, J_{HH} = 6.8 Hz, J_{PH} = 314 Hz, 1H, P*H*), 4.98 (dd, J_{HH} = 6.8 Hz, J_{PH} = 324 Hz, 1H, P*H*), 1.93 (s, 3H, CpC*H*$_3$), 1.85 (s, 3H, CpC*H*$_3$). ^{31}P-NMR (C_6D_6): δ –36.8 ppm. IR (toluene): ν(CO) 1990 (s), 1942 (s, br) cm^{-1}. Anal. Calcd for $C_{21}H_{21}Co_2Mo_2O_3PS_3$: C, 33.26; H, 2.79. Found: C, 31.24; H, 2.63. The thermal instability of the compound with respect to loss of phosphine prevented a good microanalysis.

$Cp'_2Mo_2Co_2S_3(CO)_3(PPh_2H)$. $Cp'_2Mo_2Co_2S_3(CO)_4$ (0.150 g, 0.22 mmol) was dissolved in 30 mL of toluene. PPh_2H (0.3 mL, 1.6 mmol) was added and the solution stirred overnight. Chromatography down a 25-cm column of alumina with 3:1 toluene/hexane eluted a dark brown band of $Cp'_2Mo_2Co_2S_3(CO)_3(PPh_2H)$ (0.11 g, 60% yield) followed by a small brown band of $Cp'_2Mo_2Co_2S_3(CO)_2(PPh_2H)_2$. A small green band was not eluted. ^{1}H-NMR (C_6D_6): δ 7.5 (m, 4H, Ph*H*), 7.05 (m, 6H, Ph*H*), 5.42 (m, 2H), 5.35 (m, 1H), 5.25 (m, 1H), 5.09 (m, 1H), 5.06 (m, 1H), 4.89 (m, 1H), 4.77 (m, 1H) 2ABCD pattern for Cp*H*, 5.89 (d, J_{PH} = 320 Hz, 1H, PH), 1.92 (s, 3H, CpC*H*$_3$), 1.87 (s, 3H, CpC*H*$_3$). IR (toluene): ν(CO) 1988 (s), 1941 (s, br) cm^{-1}. Anal. Calcd for $C_{27}H_{25}Co_2Mo_2O_3PS_3$: C, 38.87; H, 3.02. Found: C, 39.34; H, 3.18.

$Cp'_2Mo_2Co_2S_3(CO)_2(PPh_2H)_2$. $Cp'_2Mo_2Co_2S_3(CO)_4$ (0.129 g, 0.19 mmol) was dissolved in 30 mL of benzene. PPh_2H (0.17 mL, 0.96 mmol) was added and the solution refluxed under a slow stream of nitrogen for 3 h. Chromatography down a 20-cm column of alumina with 4:1 benzene/hexane eluted a dark brown band of a 2:1 mixture of *trans*- and *cis*-$Cp'_2Mo_2Co_2S_3(CO)_2(PPh_2H)_2$ (0.11 g, 58% yield). A small green band could not be eluted. ^{1}H-NMR (C_6D_6): *cis*-$Cp'_2Mo_2Co_2S_3(CO)_2(PPh_2H)_2$, δ 7.75 (m, 8H, Ph*H*), 7.05 (m, 12H, Ph*H*), 6.06 (d, J_{PH} = 317 Hz, 2H, P*H*), 5.57 (t, J = 2.3 Hz, 2H), 5.25 (t, J = 2.3 Hz, 2H), 5.21 (t, J = 2 Hz, 2H), 4.68 (t, J = 2 Hz, 2H) $2A_2B_2$ pattern for Cp*H*, 2.01 (s, 3H, CpC*H*$_3$), 1.91 (s, 3H, CpC*H*$_3$); *trans*-$Cp'_2Mo_2Co_2S_3(CO)_2(PPh_2H)_2$, δ 7.75 (m, 8H, Ph*H*), 7.05 (m, 12H, Ph*H*), 6.05 (d, J_{PH} = 317 Hz, 2H, P*H*), 5. 54 (m, 2H), 5.34 (m, 2H), 5.06 (m, 2H), 4.86 (m, 2H) ABCD pattern for Cp*H*, 2.00 (s, 6H, CpC*H*$_3$). IR of mixture (toluene): ν(CO) 1933 (sh), 1917 (s) cm^{-1}. Anal. Calcd for $C_{38}H_{36}Co_2Mo_2O_2P_2S_3$: C, 45.98; H, 3.65. Found: C, 46.04; H, 3.92.

Preparation of $Cp'_2Mo_2Co_2S_3(CO)_2$(DPPE). $Cp'_2Mo_2Co_2S_3(CO)_4$ (0.733 g, 1.08 mmol) and DPPE (0.746 g, 1.87 mmol) were dissolved in 50 mL of CH_2Cl_2 and refluxed for 14 h. Elution down a 25-cm column of alumina with 1:1 CH_2Cl_2/hexane yielded 0.52 g of brown product (47% yield). ^{1}H-NMR (C_6D_6): δ 7.79 (m, 4H, Ph*H*), 7.66 (m, 4H, Ph*H*), 7.0 (m, 12H, Ph*H*), 5.47 (m, 2H), 4.87 (m, 2H), 4.72 (m, 2H), 4.57 (m, 2H) ABCD pattern for Cp*H*, 2.13 (d, J_{PH} = 18 Hz, 4H, C*H*$_2$C*H*$_2$), 1.84 (s, 6H, CpC*H*$_3$). ^{31}P-NMR (C_6D_6): δ 85.9 ppm. IR (benzene): ν(CO) 1975 (s), 1927 (s) cm^{-1}. Anal. Calcd for $C_{40}H_{38}Co_2Mo_2O_2P_2S_3$: C, 47.17; H, 3.76. Found: C, 47.15; H, 3.30.

Reaction of $Cp'_2Mo_2Co_2S_3(CO)_4$ with PMe_3. $Cp'_2Mo_2Cl_2S_3(CO)_4$ (0.138 g, 0.20 mmol) was dissolved in 25 mL of CH_2Cl_2 and cooled to 0 °C. PMe_3 (0.024 mL, 0.23 mmol) was added with vigorous stirring, and the solution immediately became dark red-brown. Addition of hexane (10 mL), followed by concentration to 5 mL and cooling to –20 °C, gave dark red needles of $Cp'_2Mo_2Co_2S_3(CO)_4(PMe_3)$ (0.038 g, 85% yield). ^{1}H-NMR (C_6D_6): δ 5.06 (m, 2H), 4.95 (m, 2H), 4.83 (m, 2H), 4.80 (m, 2H) ABCD pattern for Cp*H*, 1.88 (s, 6H, CpC*H*$_3$), 0.91 (d, J_{PH} = 8.4 Hz, 9H, P(C*H*$_3$)$_3$). IR (C_6H_6): ν(CO) 1990 (s), 1956 (ms, br), 1941 (ms), 1921 (m, br) cm^{-1}. After 3 days at room temperature, the solid PMe_3 adduct reverts completely back to **1** with loss of PMe_3. An elemental analysis was therefore not attempted.

Kinetic Measurements. All kinetic experiments were run under pseudo-first-order conditions with the concentration of entering nucleophile in 10-fold excess or more.

CO Substitution Reactions of $Cp'_2Mo_2Co_2S_3(CO)_4$. Kinetic data were obtained by following the appearances of CO stretching bands of products. The IR spectra were obtained in decalin solution on a Nicolet 5PC FT-IR spectrometer using a cell with 0.2-mm NaCl windows. Constant temperatures were obtained using a Neslab RTE-8 circulating refrigeration bath. Plots of $\ln(A_\infty - A_t)$ vs time were linear over two half-lives ($r^2 > 0.995$) for all the reactions. The slopes of these lines yield observed rate constants.

PPh_3 Addition to $Cp'_2Mo_2Co_2S_3(CO)_4$. A solution of $Cp'_2Mo_2Co_2S_3(CO)_4$ in CH_2Cl_2 was mixed with PPh_3 solution at desired concentrations. The reactants and the adduct reach equilibrium instantly. The solution was syringed into a variable temperature IR cell with 0.6-mm AgCl windows, which was kept at low temperature. The low temperatures –66 and –77 °C were obtained by using $CHCl_3/CO_2$ and acetone/CO_2 baths, respectively. The reverse reaction was frozen at these temperatures, and the forward reaction was followed with IR spectrophotometry. Rate constants were obtained by plotting $\ln(A_t - A_\infty) = -k_{obsd}t$ + constant, where A is the absorbance of ν(CO) of the reactant.

CO Substitution Reactions of $Cp'_2Mo_2Co_2S_4(CO)_2$. The reaction of $Cp'_2Mo_2Co_2S_4(CO)_2$ with PPh_3 in THF yielded the monosubstituted complex, which has ν(CO) at 1948 cm^{-1}. The rate data were obtained by following the disappearance of the CO stretching band of the reactant. The sample was contained in a P/N 20.500 variable temperature IR cell with 0.6-mm AgCl windows. No kinetic intermediate was observed during the reaction.

Molecular Structure of $Cp'_2Mo_2Co_2S_3(CO)_4(PMe_3)$. A dark, rectangular plate grown from hexane/CH_2Cl_2 at –20 °C was mounted on a glass fiber and quickly transferred to the cold nitrogen stream (–100 °C) of the diffractometer. The lattice constants approximate orthor-

(18) Li, P.; Curtis, M. D. *Inorg. Chem.* **1990**, *29*, 1242.
(19) Curtis, M. D.; Williams, P. D.; Butler, W. M. *Inorg. Chem.* **1988**, *27*, 2853.

Table 1. Crystallographic Data for $Cp'_2Mo_2Co_2S_3(CO)_4(PMe_3)$ (**5**)

formula	$C_{19}H_{23}Co_2Mo_2O_4PS_3$
mol wt	752.29
color and habit	brown rectangular plate
a, b, c (Å)	7.089(1), 18.669(6), 18.469(4)
α, β, γ (deg)	90.0, 90.84(2), 90.0
vol (cm^3), Z	2448(1), 4
d ($g\ cm^{-3}$)	2.04
system, space group	monoclinic, *Pn* (no. 7)
unique rflcns	5126
no. rflcns $F_o \geq 5\sigma(F_o)$	4739
$R = \sum(\|F_o\| - \|F_c\|)/\sum\|F_o\|$	0.0404
$R_w = [\sum(w\|F_o - F_c\|^2/\sum wF_o^2]^{1/2}$	0.0500
$w^{-1} = \sigma^2(F_o) + 0.000769F_o^2$	
GOF	1.42

hombic or tetragonal symmetry, but the diffraction symmetry clearly confirmed the choice of the monoclinic lattice. No chemically reasonable solutions were found in the centric space group $P2/n$, and counting statistics strongly suggested an acentric group. Solution of the structure and refinement proceeded uneventfully in the acentric alternative, *Pn*. The correct enantiomer was determined by inversion of the coordinates and selecting the set that gave the lowest residuals. Crystal data, etc., are collected in Table 1.

Results and Discussion

Spectral Properties (General). The IR (ν_{CO}) and ^{1}H-NMR data of the Cp′ ligands are summarized in Table 2. The NMR spectra of the methylcyclopentadienyl group are especially useful in assigning stereochemistry of substitution products of $Cp'_2Mo_2Co_2S_3(CO)_4$. A "top" view of this cluster is shown in A, in which the carbonyl groups are labeled a–d. The unsubstituted cluster belongs to the C_{2v} point group, so the Cp′ resononces appear as an A_2B_2 signal (usually as a pair of pseudotriplets) and with one peak due to the equivalent methyl groups. Monosub-

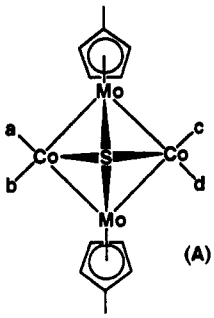

(A)

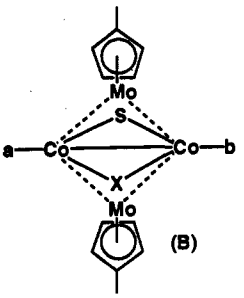

(B)

stitution at any of the equivalent sites a–d destroys all symmetry, so the Cp′ resonances appear as two ABCD sets of multiplets and the methyl groups give rise to two singlets. Disubstitution can produce three isomers by substituting the pairs of carbonyl groups labeled (a,b), (a,d), or (a,c). The (a,b) substitution pattern gives *Cs* symmetry with the two cobalt atoms lying in the mirror plane. This would produce equivalent Cp′ groups that would display one set of ABCD multiplets and one singlet for the methyl group. The (a,d) substitution pattern produces a complex with C_2 symmetry and the same type of NMR spectral pattern as for the (a,b) substitution. The (a,c) pattern again produces a *Cs* symmetry complex, but the mirror plane passes through the two molybdenum atoms. Thus, the NMR spectrum consists of two sets of A_2B_2 multiplets and two methyl group singlets. We have observed the (a,b) type substitution only with chelating diphosphines, e.g. DPPE (see Experimental Section). Thus, the NMR pattern readily distinguishes the (a,c) and (a,d) substitution patterns (hereafter called *cis* and *trans*, respectively).

Similar arguments hold for "cubane" clusters, e.g. $Cp'_2Mo_2Co_2S_3X(CO)_2$ (X = S, PR), diagrammed in **B**. If X ≠ S, and a = b, two A_2B_2 sets and two Me singlets result; if X = S and a ≠ b, then one ABCD set and one Me singlet are obtained. When X ≠ S and a ≠ b, all symmetry is removed and two ABCD sets and two Me singlets are possible.

Carbonyl Substitution Reactions. The reaction of cluster **1** with a 3-fold excess of phenylphosphine in refluxing benzene gives the monosubstituted product, $Cp'_2Mo_2Co_2S_3(CO)_3(PPhH_2)$ (**3**), after 1 h. The NMR of **3** is quite complex due to the overlap of the signals from the diasteriotopic P*H* protons with the Cp-*H* proton signals. A COSY 2-D NMR (Figure 1) allowed assignments as follows: 5.43 (H_{a1} and H_{d1}), 5.30 (H_{a2}), 5.15 (H_{d2}), 5.11 (H_{b1} and H_{c1}), 4.80 (H_{b2}), 4.62 (H_{c2}) (see diagram **C**). The large differences in the chemical shifts between the pairs H_{a2} and H_{d2} (0.15 ppm) and H_{b2} and H_{c2} (0.18 ppm) are most likely caused by the proximity of the Cp′(2) group to the ring current anisotropy of the phenyl group on the phosphine ligand.

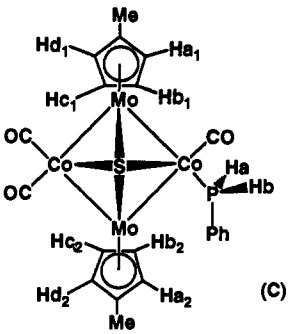

(C)

The protons, H_a and H_b, bonded to the phosphorus are also diasteriotopic. It was clear from the COSY spectrum that the peaks near 5.5 and 4.5 ppm were associated with the P-*H* protons. A spin simulation with the program PANIC allowed the determination of the coupling constants and chemical shifts: δ 4.99 and 4.98; J_{PHa} = 314 Hz, J_{PHb} = 324 Hz, J_{HaHb} = 6.8 Hz (see supplementary material).

Substitution reactions on **1** with PPh_2H are considerably faster than with $PPhH_2$. After 8 h at room temperature, the reaction of **1** with a 6-fold excess of PPh_2H forms the monosubstituted product. This complex displays two ABCD patterns at δ 5.42–4.77 and two Cp*Me* singlets. The signal for the P-*H* proton appears at δ 5.89 (J_{PH} = 320 Hz).

The monosubstituted cluster reacts further with PPh_2H in refluxing benzene to give a 3:2 mixture of cis:trans disubstituted complexes, $Cp'_2Mo_2Co_2S_3(CO)_2(PPh_2H)_2$ (**4c** = *cis*, **4t** = *trans*) (eq 2). Although we could not separate the isomers, the NMR spectrum of the mixture was easily assigned due to the different symmetries involved (see above and Table 2).

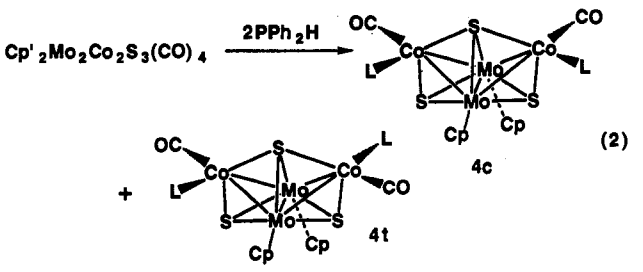

(2)

When trimethylphosphine was added to a solution of **1** at 0 °C, the color of the solution immediately changed from green-brown to deep red-brown. The ^{1}H-NMR spectrum of this solution showed the Cp′ groups to be equivalent and diasteriotopic; that is, the complex possesses a mirror plane that contains the cobalt atoms. The IR spectrum showed four ν_{CO} bands (Table 2). These spectral results are consistent with the formation of an adduct **5** (eq 3) provided that the $Co(CO)_2(PMe_3)$ vertex executes a rapid, turnstile-like rotation. The crystal structural results (see below) are consistent with a low barrier to turnstile rotation, and

Table 2. Summary of IR (ν_{CO}) and ^{1}H-NMR Data

cpd	ν_{CO} (cm^{-1})	^{1}H-NMR Cp′ protons (ppm)	
		Cp′	Me
$Cp'_2Mo_2Co_2S_3(CO)_4$	2009, m, 1987 s, 1954 ms	5.25, 4.91 (A_2B_2)	1.77
$Cp'_2Mo_2Co_2S_4(CO)_2$	1984, 1965	5.08, 4.86 (A_2B_2)	1.64
$Cp'_2Mo_2Co_2S_3(CO)_4L$			
L = PMe_3	1990 s, 1956 ms, 1941 ms, 1921 n	5.06, 4.95, 4.83, 4.80 (ABCD)	1.88
$P(OMe)_3$	1996 s, 1975 m, 1949 s, 1938 sh		
PPH_3	1990 s, 1945 ms, 1918 m		
$Cp'Mo_2Co_2S_3(CO)_3[P(OMe)_3]_2$	1965, 1947, 1929		
$Cp'_2Mo_2Co_2S_3(CO)_3L$			
L = PPh_3	1990 s, 1942 s		
PPh_2H	1988 s, 1941 s, br	5.42 (2), 5.35, 5.25, 5.09, 5.06, 4.89, 4.77 (2 × ABCD)	1.92, 1.87
$PPhH_2$	1990 s, 1942 s, br	5.43 (2), 5.30, 5.15, 5.11 (2), 4.80, 4.62 (2 × ABCD)	1.93, 1.85
P(OMe)	1993 s, 1948 s		
$P(n\text{-}Bu)_3$	1942 s, 1913 s		
$Cp'Mo_2Co_2S_3(CO)_2L_2$			
L = PPh_2H	1933 sh, 1917 s	trans: 5.54, 5.34, 5.06, 4.86 (ABCD)	2.00
	(2:1 trans:cis mixture)	cis: 5.57, 5.25, 5.21, 4.68 (2 × A_2B_2)	2.01, 1.91
$P(OMe)_3$	1949, 1940, 1927	trans: 5.78, 5.73, 5.54, 5.34 (ABCD)	2.11
		cis: 5.89, 5.59, 5.44, 5.27 (2 × A_2B_2)	2.22, 2.07
$Cp'Mo_2Co_2S_4(CO)(PPh_3)$	1948		

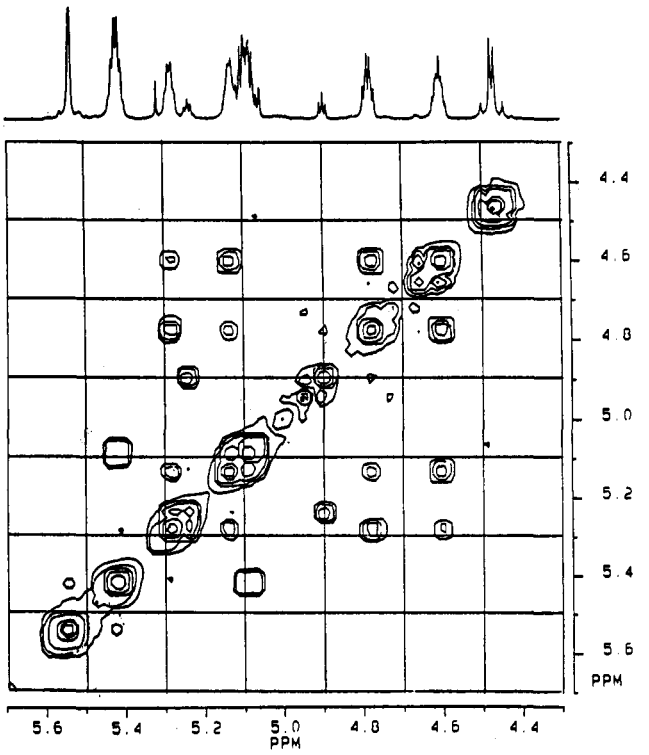

Figure 1. COSY 2-D ^{1}H-NMR spectrum of $Cp'_2Mo_2Co_2S_3(CO)_3(PPhH_2)$ (**3**) in C_6D_6.

the carbonyl groups of $M(CO)_3$ vertices are also known to rotate with low barriers.[20,21] Isocyanides also form observable adducts with **1**.[3]

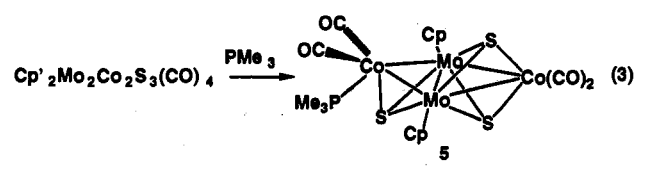

(3)

5

The adduct **5** could be isolated as an unstable solid by crystallization from a solution containing excess PMe_3 at −20 °C. On standing for several hours at room temperature, loss of PMe_3 was noticeable, and after 3 days, the loss was complete to give back cluster **1**. Carbonyl group substitution was not observed with Me_3P under these experimental conditions.

Cluster **1** reacts immediately with $P(OMe)_3$ at ambient temperature to give the adduct **1**·$P(OMe)_3$ (**6**) with a pattern of ν_{CO} frequencies and intensities similar to the adduct **5** (see Table 2). In the presence of excess $P(OMe)_3$, the adduct loses CO to form the monosubstituted product, $Cp'_2Mo_2Co_2S_3(CO)_3[P(OMe)_3]$ (**7**), but this immediately attaches another molecule of phosphite to give the $P(OMe)_3$ adduct $Cp'_2Mo_2Co_2S_3(CO)_3[P(OMe)_3]_2$ (**8**) (Scheme 1). Attempts to isolate **8** were unsuccessful; the adduct lost $P(OMe)_3$ as the solvent was pumped off, and the monosubstituted product **7** is isolated. The IR spectrum of **7** is similar to the other monosubstituted clusters (Table 2). In comparison to the IR spectra of the adducts $Cp'_2Mo_2Co_2S_3(CO)_4L$ (Table 2), the spectrum of **8** is missing the high-frequency band near 1990 cm^{-1} that is assigned to the asymmetric CO stretch of the $Co(CO)_2$ group. Thus, the adduct **8** has the structure shown in Scheme 1 as expected on the basis of both steric and electronic reasons. Complex **8** loses CO to give a mixture of *cis* and *trans* disubstituted cluster **9c** and **9t**. The fact that **9** does not react with excess $P(OMe)_3$ to give an adduct is also evidence that the structure of **8** is as shown, i.e. one phosphite ligand on each cobalt atom.

Several other clusters with different phosphines substituted for CO were prepared and spectroscopically characterized during the course of the kinetics study (see below). Their ν(CO) frequencies are listed in Table 2.

Structure of $Cp'_2Mo_2Co_2S_3(CO)_4(PMe_3)$ (5). The unit cell contained two independent molecules. Selected bond distances and angles for one of the two independent molecules are listed in Tables 3 and 4 (a complete listing is included in the supplementary material). The values of the bond distances and angles in the two independent molecules are nearly identical within experimental error. Figure 2 shows an ORTEP plot with the atomic numbering scheme; Figure 3 is an expanded view of the inner M_4S_3 core of the cluster.

Cluster **5** is derived from **1** by breaking the Co2–S2 bond and opening up the hinge angle (148° in **5** vs 125° in **1**) so that **5** appears as a tetrahedral Mo_2CoS cluster edge-fused to an Mo_2CoS_2 trigonal bipyramidal cluster (Figure 3). The Co2···S2 distance in **5** is 3.21 Å vs the Co–(μ_4-S) bond distance of 2.24 Å in **1**. The conversion of the μ_4-S ligand in **1** to the μ_3-S in **5** also shortens the remaining Co–S bond from 2.24 to 2.16 Å. However, the Mo–S bond lengths are not changed appreciably: 2.40 Å in **1** vs 2.38 Å in **5**. These changes are consistent with

(20) Braunstein, P.; Jud, J. M.; Tiripichio, A.; Tiripichio-Camellini, M.; Sappa, E. *Angew. Chem., Int. Ed. Engl.* **1982**, *21*, 307.
(21) Williams, P. D.; Curtis, M. D.; Duffy, D. N.; Butler, W. M. *Organometallics* **1983**, *2*, 165.

Scheme 1

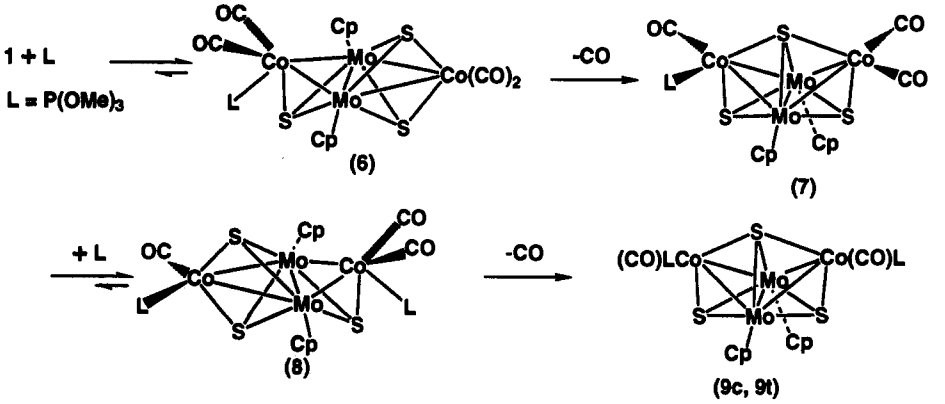

Table 3. Selected Bond Angles in $Cp'_2Mo_2Co_2S_3(CO)_4$ (PMe_3) (**5**)

bond	angle (deg)	bond	angle (deg)
Mo1–Mo2–Co1	61.36(5)	Mo2–Mo1–Co1	61.11(5)
–Co2	61.81(5)	–Co2	62.97(5)
–S1	56.90(8)	–S1	57.12(8)
–S2	57.30(7)	–S2	56.67(7)
–S3	57.48(7)	–S3	57.31(7)
Mo1–Co1–Mo2	57.53(5)	Mo2–Co1–S2	57.31(8)
–S2	57.67(8)	–S3	58.10(8)
–S3	58.11(8)	Mo2–Co2–S1	55.43(9)
Mo1–Co2–Mo2	55.22(9)	–P1	152.3(1)
–S1	55.80(8)	Mo2–S1–Co2	76.2(1)
–P1	116.9(1)	Mo2–S2–Co1	72.77(9)
Mo1–S1–Mo2	65.98(8)	Mo2–S3–Co1	71.9(1)
–Co2	75.4(1)	S1–Mo1–S2	107.1(1)
Mo1–S2–Mo2	66.03(8)	–S3	76.7(1)
–Co1	71.97(9)	S1–Co2–P1	97.4(1)
S2–Mo1–S3	91.5(1)	S2–Mo2–S3	92.0(1)
Co2–Mo1–S1	48.80(8)	S2–Co1–S3	105.1(1)
–S2	76.30(8)	P1–Co2–C15	95.1(4)
–S3	114.5(1)	–C16	94.7(4)
Co2–Mo2–S1	48.35(8)	C13–Co1–C14	97.8(5)
–S2	75.97(8)	C15–Co2–C16	105.3(5)
–S3	113.6(1)		

Table 4. Selected Bond Distances of $Cp'_2Mo_2Co_2S_3(CO)_4(PMe_3)$ (**5**)

bond	distance (Å)[a]	bond	distance (Å)[a]
Mo1–Mo2	2.594(2)	Mo1–S1	2.379(3)
Mo1–Co1	2.698(2)	Mo1–S2	2.389(3)
Mo1–Co2	2.783(2)	Mo1–S3	2.409(3)
Mo2–Co1	2.692(2)	Mo2–S1	2.385(3)
Mo2–Co2	2.813(2)	Mo2–S2	2.372(3)
Co1–S2	2.156(3)	Mo2–S3	2.405(3)
Co1–S3	2.171(3)	Co2–S1	2.164(3)
Co1–CO[b]	1.73(1)	Co2–CO[b]	1.76(1)
P1–C[b]	1.82(1)	Co2–P1	2.225(3)
Mo–C(Cp)[b]	2.36(2)	Mo–Cp[c]	1.926(2)
C–C(Cp)[b]	1.43(2)	Cp–Me[b]	1.48(3)

[a] The standard deviation of the last significant digit in parentheses. [b] Average values; the standard deviation is the greater of the values calculated from the $n-1$ formula or $(\sigma_1^2 + \sigma_2^2)^{1/2}$. [c] Mo–Cp centroid distance.

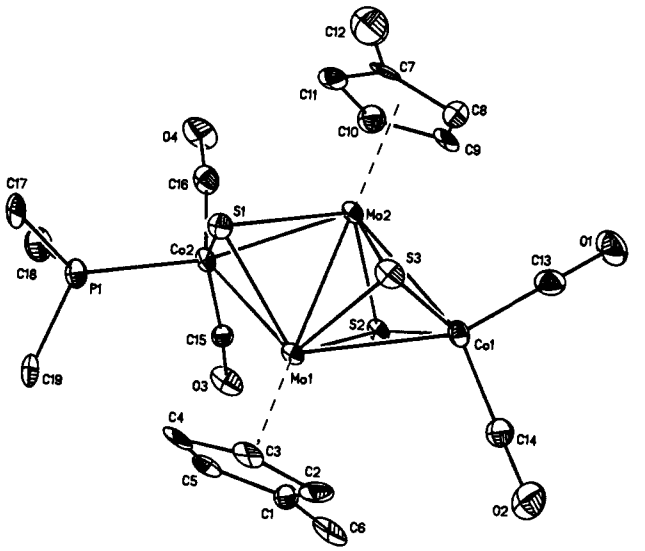

Figure 2. ORTEP diagram of $Cp'_2Mo_2Co_2S_3(CO)_3(PMe_3)$ (**5**) showing the atomic numbering scheme.

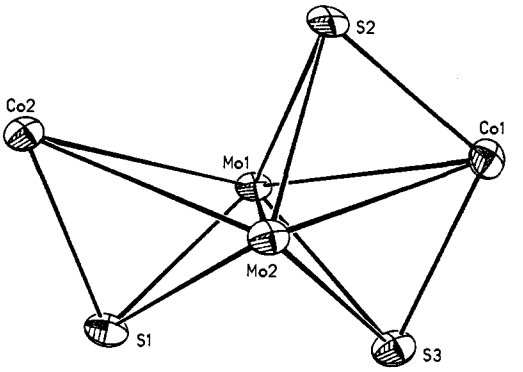

Figure 3. ORTEP diagram of $Cp'_2Mo_2Co_2S_3(CO)_3(PMe_3)$ (**5**) showing the cluster core structure.

the view of the bonding in **1** that the Mo–S bonds more nearly approximate a 2e/2c description, whereas the Co–S bonds are best described as 2e/3c.[18,19]

We have previously called attention to the fact that Mo–Mo distances in $Mo(\mu\text{-}S)_nMo$ dimers decrease appreciably as the number of bridging sulfide ligands increases.[19] The Mo–Mo bond in **5** is bridged by three μ_3-S ligands and has a distance of 2.59 Å, whereas this bond in **1**, bridged by two μ_3-S and one μ_4-S groups, is slightly longer: 2.65 Å. Surprisingly, the Co–Mo bonds in **1** are shorter: 2.64 vs 2.70 and 2.80 Å in **5**. Perhaps the electron deficient nature of cluster **1**, mostly localized on Co, causes an enhancement of the Mo–Co interaction. Note also that the Mo–Co1 bonds, bridged by two μ_3-S groups, are shorter than the Mo–Co2 bonds (one μ_3-S): 2.70 vs 2.80 Å.

The Co–C–O distances also deserve some comment. The Co–C distances averaged over both independent molecules are Co–CO: 1.76 ± 0.01 and 1.74 ± 0.01 Å for the Co with and without the Me_3P ligand, respectively. The corresponding average C–O distances are 1.15 ± 0.01 and 1.18 ± 0.01 Å. These trends suggest that the Co-atom bonded to one Me_3P ligand and one μ_3-S ligand is *less* effective in releasing electron density to the carbonyl groups than the Co-atom bonded to two μ_3-S ligands.

Kinetic Measurements. At room temperature or below, the reaction of cluster **1** with phosphorous nucleophiles gave only monosubstitution products with the concentrations and times used

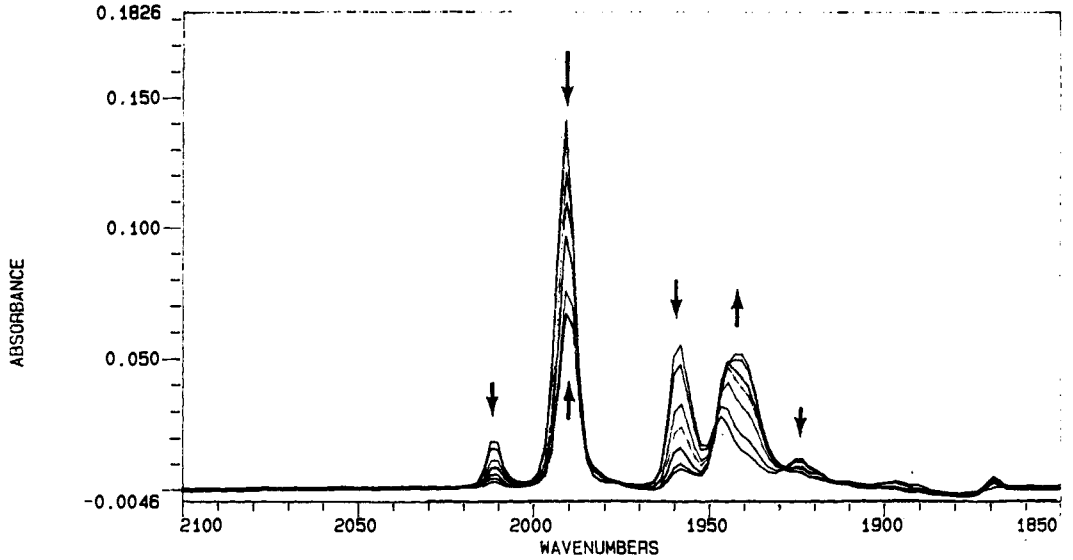

Figure 4. IR spectra (ν_{CO}) vs time for the reaction of $Cp'_2Mo_2Co_2S_3(CO)_4$ (**1**) with $PPhH_2$ in decalin.

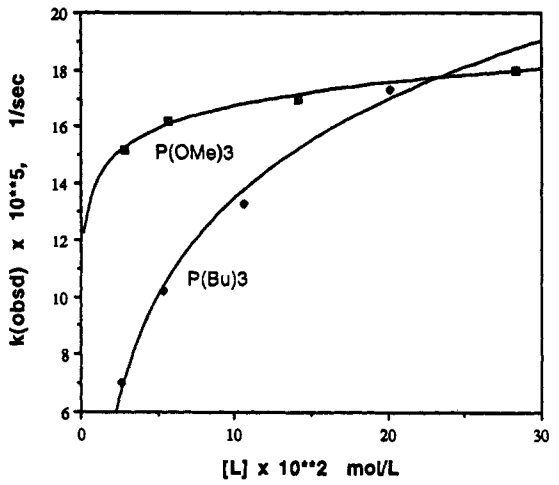

Figure 5. Plots of the observed rate constants for the reaction of $Cp'_2Mo_2Co_2S_3(CO)_4$ with $P(OMe)_3$ and $P(n\text{-}Bu)_3$ vs concentration of the ligand.

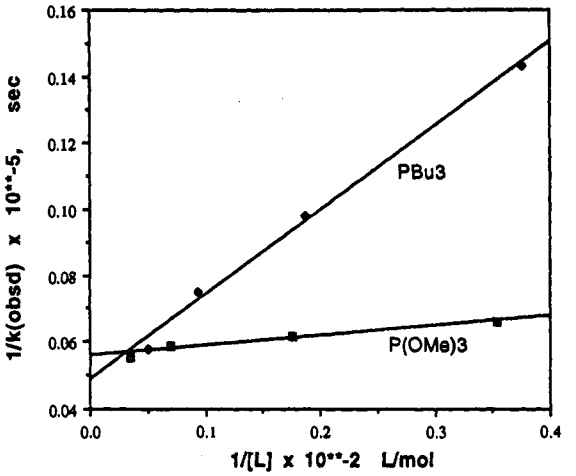

Figure 6. Plots of the inverse of the observed rate constants for the reaction of $Cp'_2Mo_2Co_2S_3(CO)_4$ with $P(OMe)_3$ and $P(n\text{-}Bu)_3$ vs the inverse of the concentration of the ligand.

for the kinetic studies. Except for the reactions with $P(OMe)_3$, rates were obtained by measuring the appearance of the $\nu(CO)$ bands of the products (Figure 4). With $P(OMe)_3$ the monosubstituted complex reacts rapidly with excess phosphite to give the adduct **8** (see above). In this case, the rate of CO substitution was measured by the appearance of the bands due to **8**. The observed first-order rate constants are given in the supplementary material.

Plots of k_{obs} vs the phosphine concentration were linear when the phosphine was PPh_2H or PPh_3. With $P(OMe)_3$ and $P(n\text{-}Bu)_3$, however, the plots suggest that k_{obs} reaches saturation at high concentrations (Figure 5). This kinetic behavior, along with the observation of adduct formation between **1** and PR_3 and other nucleophiles,[3] suggests that there is a fast preequilibrium involving formation of the adducts, followed by CO loss to give monosubstituted products (eq 4).

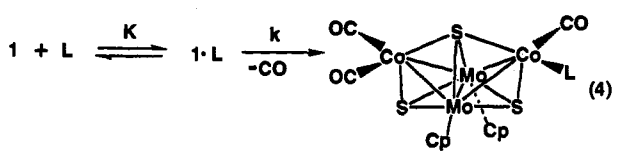

According to this mechanism, the rate law is $d[product]/dt = Kk[L]([1] + [1\cdot L])/(1 + K[L])$. Under pseudo-first-order conditions, $k_{obs} = Kk[L]/(1 + K[L])$, or $1/k_{obs} = 1/Kk[L] + 1/k$. Hence, a plot of $1/k_{obs}$ vs $1/[L]$ should be linear with slope $= 1/Kk$ and intercept $1/k$. Figure 6 shows such a plot for L = $P(OMe)_3$ and $P(n\text{-}Bu)_3$. In limiting cases, e.g. $K[L] \gg 1$, k_{obs} is nearly zero order in ligand concentration, as observed for L = $P(OMe)_3$; but when $K[L] \ll 1$, the rate law is first-order with respect to both L and cluster concentrations, as observed when L = PPh_3 and PPh_2H.

Table 5. Equilibrium and Rate Constants for the Reactions of $Cp'_2Mo_2Co_2S_3(CO)_4$ (**1**) with Phosphines

phosphine	pK_a	θ^a	T (°C)	K	$k \times 10^4$ (s^{-1})
$P(n\text{-}Bu)_3$	8.4	132	37.6	34.2	0.794
			47.0	19.1	2.06
			58.1	10.1	9.43
$P(OMe)_3$	2.6	107	8.0	230	0.546
			16.8		1.75
			26.9		7.74
PPh_3	2.7	145	37.5	0.6	5.85
PPh_2H	0.03	126	17.0	0.1	5.26

[a] Cone angle.

Table 5 shows derived values of the equilibrium constant, K, and the CO dissociation rate, k. The temperature dependence of K with $P(n\text{-}Bu)_3$ gave the following thermodynamic values: $\Delta H = -12.2 \pm 0.2$ kcal/mol, $\Delta S = -32.0 \pm 0.4$ eu, $\Delta G_{298} = -2.66$ kcal/mol, $K_{298} = 91$.

Scheme 2

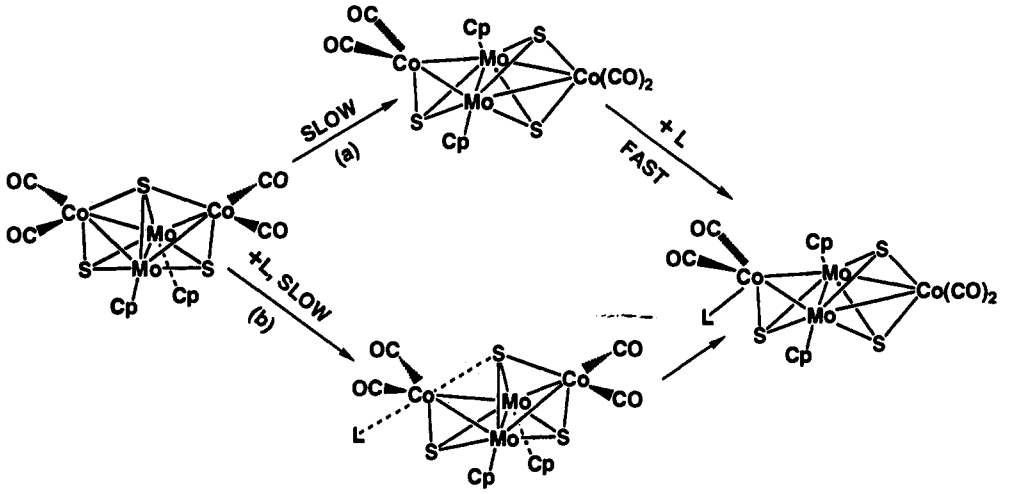

Also listed in Table 5 are the cone angles[22] of the phosphines and the pK_a of their corresponding phosphonium salts.[23] Although the equilibrium constants were determined at different temperatures, the overall trend in their values is clear. The values of the equilibrium constant appear to depend on both the basicity and the size (cone angle) of the phosphine. $P(OMe)_3$ and PPh_3 have about the same basicity, but the equilibrium constant for the former ($\theta = 107°$) is larger than that for PPh_3 ($\theta = 145°$). On the other hand, PPh_2H has a smaller cone angle ($\theta = 126°$) than $P(n\text{-}Bu)_3$ ($\theta = 132°$), but the latter phosphine has the larger equilibrium constant due to its greater basicity, $pK_a = 8.4$ for $P(n\text{-}Bu)_3$ vs 0.03 for PPh_2H.

In contrast, the rate of CO dissociation from the adduct is determined primarily by the electronic effects of the ligands. The rates decrease in the order $PPh_2H > P(OMe)_3 > PPh_3 > P(n\text{-}Bu)_3$ despite the large differences in the cone angles. A strong σ-donor ligand enhances the Co–CO bond strength, making CO displacement more difficult. The activation parameters, ΔH^* and ΔS^*, for CO displacement are 24 ± 3 kcal/mol, –0.5 ± 8 eu and 23 ± 2 kcal/mol, 3 ± 8 eu for $P(n\text{-}Bu)_3$ and $P(OMe)_3$, respectively. These data are consistent with Co–S bond formation contributing to the stability of the transition state for CO dissociation; that is, the μ_3-S helps to displace the CO as the μ_4-S bridge bond forms again.

These results leave open the question of the mechanism of *adduct* formation: does the Co–S bond break in a rate-determining step, followed by a rapid association with the phosphine (path a, Scheme 2), or does the entering nucleophile displace the Co–S bond (path b)? When **1** and PPh_3 are mixed at room temperature, the equilibrium mixture of **1** and the adduct **1**·PPh_3 is formed too rapidly to follow directly. When this equilibrium mixture is injected into an IR cell at low temperature, the equilibrium shifts toward the adduct at a rate that can be followed. The rates measured in this way show first-order dependence on phosphine concentration. The second-order rate constants, k_2, at –77 and –66 °C are 0.909 and 2.16 s^{-1} M^{-1}, respectively. The ΔH^* and ΔS^* values estimated from these two points are +5.9 kcal/mol and –28 eu, respectively. These values, along with the first-order dependence on the ligand, are consistent with path b. Path a of Scheme 2 would be expected to have a larger positive ΔH^*, and a ΔS^* either near 0 or positive.

The rate of CO displacement with PPh_3 from the cubane cluster, **2**, was measured also. The reaction was found to be first order in each reactant. The second-order rate constants, $10^3 \times k$ (T °C), are 4.21 (–23.0 °C), 10.3 (–14.0 °C), and 20.9 (–5.0 °C) s^{-1} M^{-1}. These rate constants give $\Delta H^* = 11.3 \pm 0.8$ kcal/mol and $\Delta S^* = -24 \pm 3$ eu. These data are again consistent with an associative mechanism for CO substitution, although no intermediates could be detected in this case. The reaction energy profiles for substitution on **1** and **2** are summarized in Figure 7.

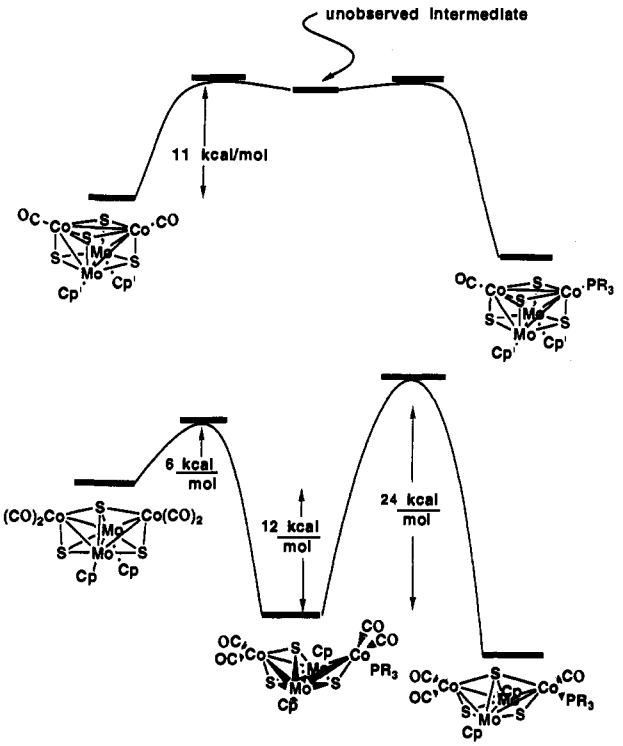

Figure 7. Composite schematic representation of the enthalpy changes vs reaction coordinate for nucleophilic CO substitution on $Cp'_2Mo_2Co_2S_3(CO)_4$ and $Cp'_2Mo_2Co_2S_4(CO)_2$.

Conclusions

The sulfido clusters $Cp'_2Mo_2Co_2S_3(CO)_4$ (**1**) and $Cp'_2Mo_2Co_2S_4(CO)_2$ (**2**) both undergo CO substitution by associative pathways. Both **1** and **2** have a valence shell electron count VSE = 60 provided the sulfur atoms act as four-electron donors. It is possible to consider cluster **1** to be a saturated 62-electron butterfly cluster if one counts the μ_4-bridging sulfur ligand as a six-electron donor. However, EHMO calculations suggest that the sulfur 3s electrons are too low in energy to contribute substantially to the bonding in the cluster.[18] A 60-electron cluster requires six metal–metal bonds for each metal to obey the 18-electron rule. Since **1** has only five metal–metal bonds, this cluster is formally electron deficient. The μ_4-sulfur ligand, which is formally bound to the

(22) Tolman, C. A. *Chem. Rev.* **1977**, *77*, 313.
(23) Rahman, M. M.; Lui, H. Y.; Eriks, K.; Prock, A.; Giering, W. P. *Organometallics* **1989**, *8*, 1.

two cobalt atoms with a delocalized 3c,2e bond[18] in **1**, is transformed to a μ_3-ligand with localized 2c,2e bonds in the 62-electron adducts **1**·L. Thus, addition of two electrons in the formation of the adducts **1**·L converts **1** to an electron-precise butterfly that has sufficient stability to be isolated and completely characterized. Although **2** does not form a stable adduct, the transition state can be stabilized by the formation of an intermediate with either 60 or 62 electrons. Breaking a Co–S bond in **2**·L converts a 4*e*-donor μ_3-sulfide to a 2*e* μ_2-S and keeps the electron count at 60. On the other hand, a Co–Co bond can break, and in this case a precise 62-electron butterfly is formed. The ability of the heterobimetallic clusters to readily coordinate ligands may contribute to their unique desulfurization activity.

Acknowledgment. M.D.C. thanks the National Science Foundation for support of this research under Grant CHE-9205018. O.J.C. also thanks the Horace H. Rackham School of Graduate Studies and the Department of Chemistry for Yates and Riggs Fellowships. F.B. and J.K.S. thank the National Science Foundation Grant CHE-8818696 and a Northwestern University Presidential Grant for the support of this research.

Supplementary Material Available: Figures showing the numbering scheme for both independent molecules in the unit cell of **5** and the calculated and observed ^{1}H-NMR spectrum in the Cp and P-H region for **3** and tables of crystal data collection and refinement information, atomic coordinates, anisotropic thermal parameters, H-atom coordinates, bond distances and angles, and observed rate constants (22 pages); tables of observed and calculated structure factors for **5** (19 pages). This material is contained in many libraries on microfiche, immediately follows this article in the microfilm version of the journal, and can be ordered from the ACS; see any current masthead page for ordering information.